Photonic Crystals for Hyper-Raman Technique to Fast Diagnose of COVID-19 Even in Traces and to Break Down Coronavirus Activity Through a Destroying Natural Oscillations of SARS-CoV-2 Ribonucleic Acid

BI DongXue[1,2], Vladimir FILATOV[2*], Anna KARADZIC[2] and WU MengYuan[1,2]

[1]Lebedev Physical Institute of Russian Academy of Sciences, Russia

[2]Bauman Moscow State Technical University, Russia

[*]vvfilatov@bmstu.ru,

Abstract. The dynamics of COVID-19 cases in Europe shows a novel coronavirus SARS-CoV-2 is able to photoactivate by a natural solar radiation. This means, there are optical-sensitive modes in a spectrum of natural oscillations of the RNA. This paper analyses the dynamics of RNA optical electrons to determine spectral location of the optical-active modes. To do it, we perform the model-independent estimation (what is correct for all varieties of SARS-CoV-2, both known and new ones) as well as model-dependent simulation reveal the location of RNA optical-active modes at several GHz. This allows to use Raman scattering to detect the presence of COVID particles in the ambient air or in a patient saliva sample for fast diagnosis the infection. To enhance Raman signal, we propose to use the photonic crystal as an active Raman substrate. This way, the giant density of optical Tamm states at photonic crystal bandgap edges can be used to resonantly amplify the local (near surface) electromagnetic field to detect a presence of SARS-CoV-2 virions even in traces. This photonic crystal scheme allows to make a portable test device to not only express-diagnose COVID-19 with an ultimate precision, but also to destroy natural oscillations of coronavirus RNA and break down virus activity. This makes possible to kill the virus inside a human body by an optical way.

Introduction

Severe acute respiratory syndrome coronavirus 2 (SARS-CoV-2, formerly known as 2019-nCoV) is a one-chain (+) ribonucleic acid (RNA) spherical virus resulting to COVID-19 decease. The correlation between COVID-19 cases in Europe with a local level of a natural solar radiation shows SARS-CoV-2 is able to photoactivate [1]. The theoretical investigations [2] describes this as a natural optical stimulation of the RNA optical-active modes what are determines the virulence. Since there is an optical way to stimulate the virus, this one can also be used to overstimulate it to turn the virus off.

Analysis

Model-Independent Simulation. Because of fast evolution, the virus itself is very changeable, so to deal with all SARS-CoV-2 varieties (both known and new ones), one should use the model-independent method. Since SARS-CoV-2 is a spherical virus about $D \approx 0.1\ \mu m$ in a diameter, the optical electrons of its RNA (what determine the RNA's optical-active modes) are localized in the region with the characteristic size of $\Delta x \approx D$. This way, the Heisenberg uncertainty relation

$$(\Delta x) \times (\Delta p_x) \gtrsim \hbar \tag{1}$$

gives the following uncertainty of the momentum for the RNA optical electron

$$(\Delta p_x) \gtrsim \frac{\hbar}{(\Delta x)} \approx \frac{\hbar}{D} \tag{2}$$

and can be used to estimate the momentum itself. Actually, because $\Delta p_x \approx p$, we get

$$p \gtrsim \frac{\hbar}{D} \tag{3}$$

what gives the estimation for the kinetic energy of electron (with mass $m_e = 9.1 \times 10^{-31}\, kg$) as

$$W = \frac{p^2}{2m_e} \gtrsim \frac{\hbar^2}{2m_e D^2}. \tag{4}$$

This way, electronic transitions in RNA correspond to the electromagnetic radiation of frequencies

$$\omega = \frac{\Delta W}{\hbar} \approx \frac{W}{\hbar} \approx \frac{\hbar}{2m_e D^2} \approx \frac{10^{-34}}{10^{-30} \times 10^{-14}} \approx 10^{10}\, rad/s, \tag{5}$$

i.e. gigahertz ($\nu \approx 10^9\, Hz$) ones.

Model-Depended Simulation. To precise estimations (5), we assume the RNA of SARS-CoV-2 is a ball of "spaghetti" what is encapsulated inside the spherical lipid membrane. This means the RNA optical electron is located in a ball quantum well. Since this,

$$U(r) = \begin{cases} 0,\, inside\,(r < D/2) \\ \infty,\, outside\,(r > D/2) \end{cases} \tag{6}$$

Inside the well we gauge the potential energy to zero, outside the well we assume the energy is infinity to not allow electron to leave RNA (otherwise, the RNA becomes a free radical and spontaneously collapses).

For this potential energy, the Schrodinger equation for the RNA optical electron is the following:

$$\left[\frac{-\hbar^2}{2m_e} \nabla^2 + U(r) \right] \psi(\vec{r}) = W\psi(\vec{r}), \tag{7}$$

where ψ is an electron wavefunction. Because of spherical symmetry, the equation simplifies to

$$\frac{-\hbar^2}{2m_e} \left[\frac{1}{r} \frac{d^2}{dr^2} (r\psi(r)) \right] = W\psi(r) \tag{8}$$

and furthermore to

$$(r\psi)'' = \frac{-2m_e W}{\hbar^2} (r\psi). \tag{9}$$

To satisfy the border condition ($\psi = 0$ at $r = D/2$), one should solve (9) as

$$\psi(r) = A \frac{\sin[k(r - D/2)]}{r}, \tag{10}$$

with $k = \hbar^{-1} \times (2m_e W)^{1/2}$.

The continuity condition for ψ-function at $r \to 0$ gives

$$k \times D/2 = \pi n, n \in N \tag{11}$$

resulting to the electron energies

$$W \equiv W_n = \frac{(2\pi\hbar n)^2}{2 m_e D^2} = \frac{h^2}{2 m_e D^2} n^2, n \in N \tag{12}$$

and its natural frequencies

$$v_n = \frac{W_n}{h} = \frac{h}{2 m_e D^2} n^2, \tag{13}$$

where $h = 6.6 \times 10^{-34}$ $J \times s$ is Planck constant and $n = 1, 2, 3...$

Finally, the RNA optical spectrum is

$$v_{mn} = \frac{W_n - W_m}{h} = \frac{h}{2 m_e D^2}\left(n^2 - m^2\right), \tag{14}$$

where m and n are natural numbers.

Low-Frequency Raman Scattering. The calculated frequencies (13) and (14) can be used to detect a presence of virus particles by an optical way. This way, the peaks intensities give the concentration of virions to early diagnosis the disease. To do this, there are two standard techniques: direct GHz-spectroscopy and Raman scattering. The experiments with nucleic acids [3] and SARS-CoV-2-similar plant virus [4] confirm that nucleic GHz frequencies (5) are detectable by a standard laboratory Raman spectrometer. This case, to compact the device, we propose to use the intracavity [5] stimulated Raman technique based on a photonic crystal [6] to realize the scheme in a single chip [7].

Photonic Crystal. Photonic crystal is an artificial metamaterial with a periodical superlattice resulting to photonic bandgaps in the visible spectrum [8]. Nowadays, the best of it is the anodic aluminum oxide (AAO) one made by the aluminum oxide (Al_2O_3) which was periodically etched by a hydrofluoric acid (HF) during anodization [9]. SEM image of crystal (see fig. 1) reveals optical cavities (pores) to obtain Bose-Einstein condensation (BEC) of light [10] inside to form a giant local electromagnetic field stimulating light scattering.

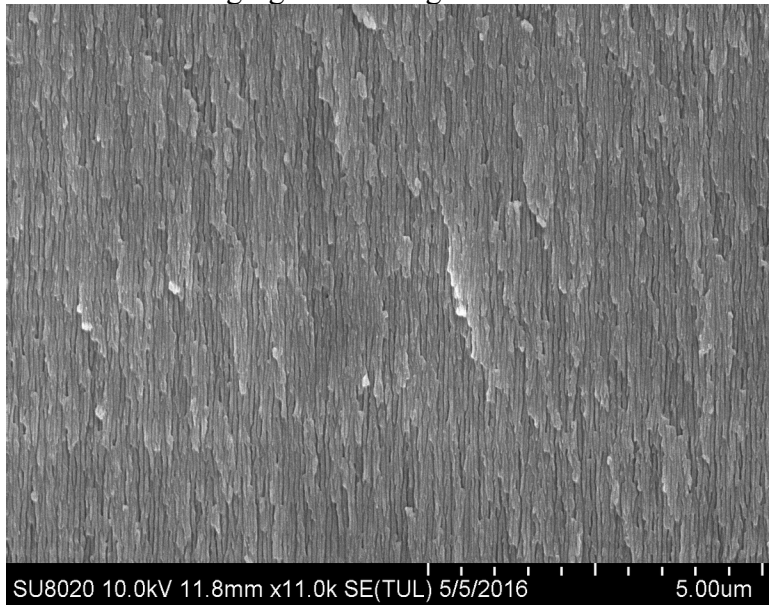SU8020 10.0kV 11.8mm x11.0k SE(TUL) 5/5/2016   5.00um

Fig. 1. SEM image of the slice of AAO photonic crystal. Note many vertical cylindrical microcavities going through the crystal because of controlled etching during anodization.

Because of the synthesis technology, photonic crystal has the most regular structure alongside the direction of its grow. Since this, the crystal should be used alongside this direction. This makes the real three-dimensional (3D) photonic crystal acts as the effective one-dimensional (1D) one. This way its superlattice is the 1D effective Bragg stack of regularly alternating layers, wherein all the odd layers are the same, as well as all the even ones.

For this 1D periodical structure, the Bloch-Floquet formalism gives the following dispersion equation for a light propagating within [11]:

$$\cos(ka) = \cos(k_1 a_1) \times \cos(k_2 a_2) - \frac{1}{2}\left(\frac{n_1}{n_2} + \frac{n_2}{n_1}\right) \times \sin(k_1 a_1) \times \sin(k_2 a_2). \tag{15}$$

Here index $i = 1$ designates the odd layers, $i = 2$ for the even ones, a_i are thicknesses, n_i are refractive indices, $k_i = \omega \times n_i/c$ are wavenumbers, $a = a_1 + a_2$ is the period of the structure, ω is the frequency of a propagating electromagnetic wave and $c = 3 \times 10^8$ m/s is the speed of light in a void.

The solution for (15)

$$k(\omega) = \frac{1}{a_1 + a_2} acos\left\{\cos\left(\frac{\omega n_1}{c} a_1\right) \times \cos\left(\frac{\omega n_2}{c} a_2\right) - \frac{1}{2}\left(\frac{n_1}{n_2} + \frac{n_2}{n_1}\right) \times \sin\left(\frac{\omega n_1}{c} a_1\right) \times \sin\left(\frac{\omega n_2}{c} a_2\right)\right\} \tag{16}$$

gives photonic bandgaps (areas of no solution) at the critical point of Brillouin zone ($k = \pi/a$) as well as at its center ($k = 0$). Inside the bandgaps light cannot propagate in the crystal, and at bandgap edges the group speed of light

$$v(\omega) = \frac{d\omega}{dk} = \left[\frac{dk(\omega)}{d\omega}\right]^{-1} \tag{17}$$

is equal to zero. This means the light of frequency matched to the bandgap edge penetrates into the crystal only at a depth of its wavelength, then stops [12]. The resulting localized standing wave is BEC [13]. Actually, the local density of states

$$\rho \propto \frac{1}{v} = (v \to 0) = \infty \tag{18}$$

resulting to the resonant amplification of a local field:

$$E(\omega) = \frac{E_0(\omega)}{\varepsilon(\omega)} = \frac{E_0(\omega)}{n^2(\omega)} = \frac{E_0(\omega)}{[c \times k(\omega)/\omega]^2} = \infty, \tag{19}$$

where E_0 is the electric field of a source, ε is the dielectric function and n is the effective refractive index of the crystal.

Finite-difference time-domain (FDTD) numerical simulation also confirms the prediction (19): the bandgap edge-matched light forms BEC at the nearest-to-surface photonic crystal microcavity (see fig. 2 and our paper [14] for details).
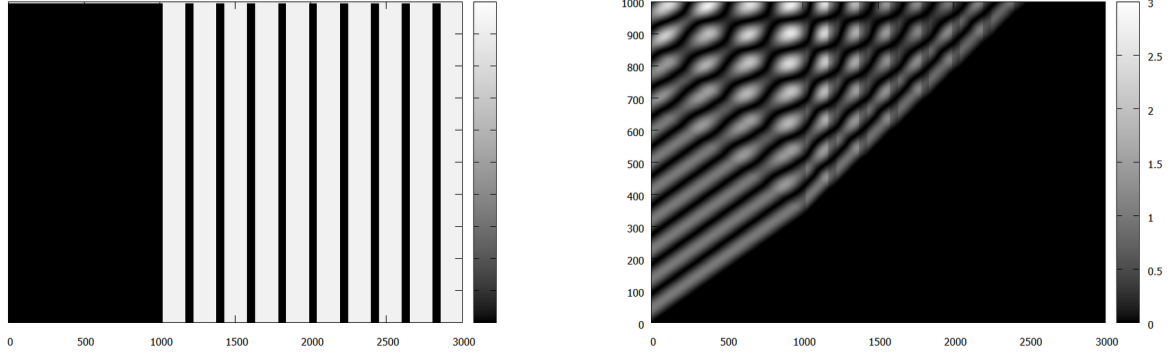
<center>(a)   (b)</center>

Fig. 2. Refractive index distribution inside the photonic crystal (fig.a, n is in arbitrary units) resulting to formation of surface optical Tamm states (fig.b, local energy is in a.u.). At fig. a and b, abscissa is a coordinate inward the crystal (a.u.); at fig.b ordinate is time (a.u.). For details see [14].

Fano Resonance for the Photonic Crystal Bandgap Edge BECs. Since photonic crystal has several BEC frequencies, one can use it to obtain its interference (Fano resonance) resulting to the amplification of the mean frequency as well as low frequency envelope:

$$E(\omega_1) + E(\omega_2) = E_0 \cos(\omega_1 t) + E_0 \cos(\omega_2 t) = 2E_0 \cos(\omega_{low} t) \times \cos(\omega_{high} t), \qquad (20)$$

where $\omega_{high} = (\omega_1 + \omega_2)/2$ is the mean frequency and $\omega_{low} = (\omega_2 - \omega_1)/2$ is the spectral half-difference between BECs. Note, the mean frequency corresponds to the bandgap center and gives the maximum reflectance, so it can be calculated via Bragg law

$$2an = \lambda = \frac{2\pi c}{\omega} \qquad (21)$$

giving

$$\omega_{high} = \frac{\pi c}{an} \simeq \frac{\pi c/a}{\sqrt{(a_1/a)n_1^2 + (a_2/a)n_2^2}}. \qquad (22)$$

The low-frequency ω_{low} is the halfwidth of a photonic bandgap, so it equals [11] to

$$\omega_{low} = \frac{\Delta\omega}{2} = \frac{1}{\pi}\omega_{high}\frac{\Delta n}{n} \simeq \frac{\omega_{high}}{\pi}\frac{|n_2 - n_1|}{\sqrt{(a_1/a)n_1^2 + (a_2/a)n_2^2}}. \qquad (23)$$

Besides of ω_1 and ω_2, it is also possible to use ω_{high} and ω_{low}.

Discussion

The results allow to calculate the photonic crystal parameters to obtain BEC at coronavirus RNA frequencies (5). To do this, one should use the photonic crystal with period of

$$a \simeq \frac{\pi c}{\omega_{high} n} \approx \frac{10^9}{10^{10}} \approx 10^{-1} m \qquad (24)$$

(see Bragg law (22)). This can be easy realized. Besides, to make the device more compact, we propose to use ω_{low} of the low-contrast ($\Delta n/n \approx 10^{-2}$) AAO photonic crystal film with $a \approx 10^{-3}$ m.

<center>5</center>

Broadband Excitation. To cover a wide range of frequencies, we also propose to use a gradient photonic crystal (with gradient of layer thickness). This way, the excited spectrum is [15]

$$R(\omega) = \int_{a_{min}}^{a_{max}} R(\omega, a)\, p(a)\, da = \frac{1}{a_{max} - a_{min}} \int_{a_{min}}^{a_{max}} \left[\frac{k(\omega) - \omega/c}{k(\omega) + \omega/c} \right]^2 da, \qquad (25)$$

where crystal period a uniformly varied from a_{min} to a_{max}. This allow to excite a wide range of polar RNA modes to randomize its natural oscillations and tune the RNA off.

Fiber Optic Device. Since optical BEC in the photonic crystal forms near to the crystal surface (see fig. 2), there is an opportunity to deliver its high-energy (19) optical Tamm states of resonant frequency [16] directly to the infected area (to minimize by-effects) inside a patient's body via optical fiber (fig. 3). When it realized as a wrist-worn gadget, the device can be used to purify the blood over virus particles.
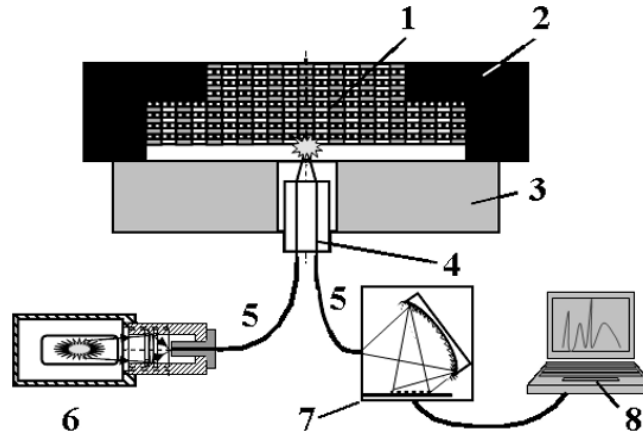

Fig. 3. Proposed scheme to obtain optical BEC and deliver it by an optic fiber (figure is from our paper [17]). Here, the photonic crystal *1* is fixed in a case *2* covered by a fluoroplastic plate *3* with a window *4* to Bose-condense a light delivered by an optical fiber *5* from an optical source *6*. At the figure, there also are digital spectrometer *7* and PC *8* to test the device.

Conclusion

The results show an opportunity not only to detect (via surface-enhanced Raman scattering) but also inhibit (via GHz-jamming of RNA) and even kill (by the over-excitation resulting to the RNA destruction) SARS-CoV-2 virions by an optical way. To do it, we propose to use the photonic crystal based hyper-Raman scheme (see fig. 3) which can be realized on a single chip.

At the moment of revision of the article, the electromagnetic suppression of coronavirus RNA is independently realized in a GHz-jammer performing very well [18]. There also are good results from an infrared laser what over-excites the RNA to destruct its secondary and tertiary structures [19].

Acknowledgments

References

[1] D.A. Poletaev, B.V. Sokolenko, Possibility of COVID-19 virion's photoactivation, Proceedings of X International conference on photonics and information optics (Russia, 2021) 323-324

[2] B.L. Ihlov, Spectra of DNA. Review, Journal of new medical technologies 25 (2) (2018) 121-134

[3] M.A. Shevchenko et al, Stimulated low-frequency Raman scattering in albumin, Journal of Russian laser research 40(1) (2019) 71-75

[4] O.V. Karpova et al, Stimulated low-frequency Raman scattering in brome mosaic virus, Journal of Russian laser research 42(1) (2021) 106-113

[5] M.A. Shevchenko et al, Intracavity stimulated low-frequency Raman scattering, Bulletin of the Lebedev physics institute 45(12) (2018) 397-398

[6] M.A. Shevchenko et al, Stimulated Raman scattering in photonic crystals infiltrated with Raman-active liquids, Journal of Russian laser research 40(6) (2019) 554-558

[7] K. Sugioka and S. Bai, 3D microfluidic SERS chips fabricated by hybrid femtosecond laser processing for attomolar sensing, Proceedings of V International conference on ultrafast optical science (Russia, 2021) 217

[8] S.M.Rytov, Electromagnetic properties of a finely stratified medium, Soviet physics JETP 2 (1956) 466-475

[9] V.S. Gorelik et al, Transmission spectra of one-dimensional porous alumina photonic crystals, Photonics and nanostructures - fundamentals and applications 32 (2018) 6-10

[10] J. Klaers et al, Bose–Einstein condensation of photons in an optical microcavity, Nature 468 (2010) 545-548

[11] A. Yariv, P. Yeh, Optical waves in crystals: propagation and control of laser radiation, Wiley, 2002

[12] V.S. Gorelik et al, Optical characteristics of the aluminium mesoporous photonic crystal, Journal of physics: conference series 1348(1) (2019) 012059

[13] S.V. Pichkurenko, Dispersion of light in the 1D photonic crystal, IOP conference series: Materials science and engineering 859(1) (2020) 012003

[14] S.V. Pichkurenko, V.V. Filatov, Localization and amplification of the electromagnetic field in a globular photonic crystal, Physics of atomic nuclei 82(12) (2019) 1672-1673

[15] V.S. Gorelik, V.V. Filatov, Spectroscopy of stop bands of globular photonic crystals filled with water, Bulletin of the Lebedev physics institute 39(11) (2012) 311-319

[16] Bi DongXue et al, Globular photonic crystal as a perspective medium for the surface-enhanced Raman scattering, Proceedings of VII International conference on laser and plasma research and technologies (Russia, 2021) 1 205-206

[17] V.S. Gorelik et al, Mesoporous photonic-crystal films for amplification and filtering of electromagnetic radiation, Journal of Russian laser research 37(6) (2016) 604-610

[18] Material from the site https://torvolna.ru/en

[19] S.N. Shelygina et al, Laser-based inactivation method of pathogenic microorganisms, Proceedings of V International conference on ultrafast optical science (Russia, 2021) 255